Pramana – J. Phys. (2022) 96:164
https://doi.org/10.1007/s12043-022-02417-9

Total excitation energy distribution for neutron-induced fission of thorium isotopes

P MEHDIPOUR KALDIANI* and M JAMIATI

Department of Physics, Naragh Branch, Islamic Azad University, Naragh, Iran
*Corresponding author. E-mail: payammehdipour@gmail.com

MS received 11 December 2020; revised 2 April 2022; accepted 11 April 2022

Abstract. The fission fragment total excitation energy, TXE(A), was calculated for neutron-induced fission of $^{227-233}$Th using three methods. The first method is the conventional method of calculating TXE by subtracting Q value from total kinetic energy value. The second method is usually used to calculate the number of neutrons emitted and the third method is a systematic method by applying the intrinsic energy within the statistical scission point model. Third method has been modified based on the results of the other two methods and the required parameters have been obtained from neutron-induced fission of ^{232}Th to calculate TXE distribution for other thorium isotopes. This indicates that for all thorium isotopes, TXE values increase with increasing mass numbers of fission fragments, except for the fission fragments with mass number about 95–100.

Keywords. Statistical scission point model; total excitation energy; neutron-induced fission; fission fragments.

PACS Nos **25.85.Ec; 26.40.−k; 24.10.−i**

1. Introduction

The investigation of energy in the fission process is essential to measure some quantities, such as the number of prompt neutrons etc. Because of these applications, kinetic energy for many reactions has been studied since the 1970s. In particular, the use of neutron-induced fission of ^{232}Th in nuclear weapons and reactors has encouraged many researchers to measure the kinetic energy of this reaction [1–4]. The total energy available in the fissioning system is stored in the form of excitation energy and kinetic energy [5]. In all studies, only the total kinetic energy (TKE) has been studied. Since excitation energy is an intrinsic energy, it cannot be measured directly. So it has been rarely studied. The only isotope of thorium whose kinetic energy has been measured is ^{229}Th [6,7]. Since there is no available data on TXE(A) for other thorium isotopes, TXE for thorium isotopes is investigated in this study.

Temperature and level density parameter of fission fragments have been calculated by determining TXE [8]. Also, deformation energy and deformation parameters of the fragments have been calculated by obtaining TXE values [5]. Of course, the most important quantity that can be calculated using TXE values is the neutron multiplicity of fission fragments ($\nu(A_i)$). Faust [9] calculated TXE distribution for ^{258}Fm fission. By comparing his results with the TXE distribution for light actinide fission, it can be concluded that the shape of the TXE distribution depends on the fission mode.

The first method is the simplest method in which the total excitation energy (TXE) is the difference between the Q-value and TKE value. In some studies [8,10–13], the binding energy and the excitation energy of fissioning nucleus (E_{cn}) have been added. On the other hand, the total prompt neutron multiplicity (ν_T) can be evaluated by TXE value at low excitation energy [14]. Ruben *et al* [15] have calculated neutron multiplicity as a function of fission fragment mass numbers, $\nu(A)$, for ^{237}Np neutron fission. Lang *et al* [16] have calculated $\nu(A)$ with three sets of different experimental data and compared them with the results calculated using Method 1 for ^{235}U thermal-neutron fission. Schmitt *et al* [17] and Neiler *et al* [18] also compared the results of these two methods for ^{235}U, ^{239}Pu, ^{241}Pu thermal-neutron fission and ^{252}Cf spontaneous fission. In the second method, we evaluate TXE(A) by using $\nu(A)$. Unfortunately, $\nu(A)$ is rarely studied for thorium isotopes. Only Visan *et al* [19] have evaluated $\nu(A)$ for ^{232}Th fission. Therefore, for other thorium isotopes, the TXE distribution cannot be evaluated by the second method. The last method is based on the static model. In this method (Method 3),

Published online: 30 August 2022

TXE can be calculated by adding deformation energy and intrinsic energy. By comparing the results of this method with the results of the other methods, we can see that this method is an improved version. In ref. [20], a similar method is used to calculate TXE for uranium isotopes. In this study, the height of the outer fission barrier and the dissipative energy are used instead of the intrinsic energy. Based on the dynamic model, Carjan *et al* [21] obtained TXE values with deformation energy during the neck rupture and after scission. Also, Ivanyuk [22] evaluated the magnitude of the total excitation energy of the fission fragments using the maximal elongation at which the nucleus splits into two fragments.

After investigating the fission fragment mass distribution [23,24] and the TKE distribution [25–27] using the modified scission point model, the TXE distribution is evaluated here using this model. In this model, the scission configuration is assumed to consist of two spheroidally shaped fragments. The distance between the two spheres is s and the Coulomb repulsion energy between them indicates the Coulomb potential energy of the system at the scission point. The deformation parameters of fission fragments are taken as quadratic in radius change (β_i; i = L, H for the light and heavy fragments, respectively). The third method is a systematic scission point model. The advantage of this method is that TXE values are evaluated systematically and calculations are not performed separately for each fission fragment.

In §2, three methods are introduced for calculating TXE. In the next section, the calculated results of these three methods for thermal neutron fission of ^{232}Th are compared and their behaviour is discussed. Then, the total excitation energy distribution is presented for neutron-induced fission of all thorium isotopes.

2. Theoretical framework

The basic energy balance equation describes all partition available energy as

$$Q(A_{\rm L}/A_{\rm H}) + E_{cn} = E_{\rm pre} + E_{\rm Coul}(A_{\rm L}/A_{\rm H}) + E_{\rm def}(A_{\rm L}, A_{\rm H}) + E_{\rm dis} + E_h, \quad (1)$$

where $A_{\rm L}$ and $A_{\rm H}$ are the mass numbers of the light and heavy fission fragments, respectively. $E_{\rm Coul}(A_{\rm L}/A_{\rm H})$ is the Coulomb potential energy at scission, $E_{\rm def}(A_{\rm L}, A_{\rm H})$ is the deformation energy of the light and heavy nascent fragment at scission. $E_{\rm dis}$ and E_h are the dissipative energy and the intrinsic excitation, respectively. $E_{\rm pre}$ is the pre-scission kinetic energy and E_{cn} is the initial excitation energy of the fissioning nucleus. The Q-value for each probable fission fragment is defined as

$$Q(A_{\rm L}/A_{\rm H}) = M(A, Z) - \sum M(A_i, Z_i), \quad (2)$$

where $M(A, Z)$ and $M(A_i, Z_i)$ are the mass excesses of the compound nucleus and the complementary fission fragments, respectively. Also, the atomic number of fission fragments is calculated by the most probable charge based on the unchanged charge-density distribution as [28]

$$Z_{\rm UCD} = \frac{Z_{cn}\,(A+\nu)}{A_{cn}}, \quad (3)$$

where ν is the post-scission neutrons [29,30].

2.1 *Method* 1

Total excitation energy is the difference between the Q value of fission and the total kinetic energy of complimentary fragments as [5,15,17,18]

$$\mathrm{TXE}(A_{\rm L}, A_{\rm H}) = Q(A_{\rm L}/A_{\rm H}) + E_{cn} - \mathrm{TKE}(A_{\rm L}/A_{\rm H}). \quad (4)$$

In many studies [8,11], the neutron binding energy of fissioning system (B_n) is added in eq. (4) as

$$\mathrm{TXE}(A_{\rm L}, A_{\rm H}) = Q(A_{\rm L}/A_{\rm H}) + B_n + E_{cn} - \mathrm{TKE}(A_{\rm L}/A_{\rm H}). \quad (5)$$

2.2 *Method* 2

In this method, the prompt neutron multiplicity of fragment $\nu(A_i)$ is used to calculate TXE as

$$\mathrm{TXE}(A_i) = \nu(A_i)(B_n(A_i) + \varepsilon(A_i)) + E_\gamma(A_i), \quad (6)$$

where $E_\gamma(A_i)$ is the average gamma energy emitted. According to [31], we have $E_\gamma(A_i) = 0.36A_i + 4.4$. $B_n(A_i)$ is the neutron binding energy of fragment A_i. Also, the average energy in the centre mass system, $\varepsilon(A_i)$, is $\frac{3}{4}(\frac{\mathrm{TXE}}{a(A_i)})^{1/2}$ [10,32]. The level density parameter, a, is obtained by [33]

$$a(A_i) = \tilde{a}(A_i)(1 + E_{\rm shell}(1 - \mathrm{e}^{-0.05\,E_{cn}})/E_{cn}), \quad (7)$$

where $E_{\rm shell}$ is the shell correction energy and we have [34]

$$\tilde{a}(A_i) = 0.0984\,A_i - 0.253\,{A_i}^{2/3} + 2.07\,\sqrt[3]{A_i} - 4.04. \quad (8)$$

2.3 *Method* 3

Total kinetic energy is usually calculated as [15]

$$\mathrm{TKE}(A_{\rm L}/A_{\rm H}) = E_{\rm Coul}(A_{\rm L}/A_{\rm H}) + E_{\rm pre}. \quad (9)$$

In this way, eq. (1) can be rewritten as

$$Q(A_L/A_H) + E_{cn} - \mathrm{TKE}(A_L/A_H) = E_{\mathrm{def}}(A_L, A_H) + E_{\mathrm{dis}} + E_h. \quad (10)$$

Since the fragment intrinsic energy, $E_{\mathrm{int}}(A_L, A_H)$, is sum of the dissipative energy and the intrinsic excitation energy, and by comparing eq. (10) with eq. (4), we have

$$\mathrm{TXE}(A_i) = E_{\mathrm{def}}(A_L, A_H) + E_{\mathrm{int}}(A_L, A_H). \quad (11)$$

The intrinsic energy and deformation energy are expressed below.

The deformation energy of fragments can be defined by minimising the nuclear potential in deformation space as [15,35]

$$E_{\mathrm{def}} = \frac{E_{\mathrm{Coul}}^4}{4\alpha e^2 Z_1^2 (Z - Z_1)^2}, \quad (12)$$

where α is the deformability parameter of each fragment. Terrell [35] presented a simple relation in the liquid drop model. Thus, α can be roughly evaluated using the following approximate relation [26]:

$$\alpha = 4.86 - 0.063\frac{Z^2}{A}. \quad (13)$$

Also, the Coulomb energy is calculated as [36,37]

$$E_{\mathrm{Coul}} = \frac{Z_1 Z_2 e^2}{D}\left(1 + 0.3785\frac{R_2^2\beta_2 + R_1^2\beta_1}{D^2} + 0.1364\frac{R_1^2\beta_1{}^2 + R_2^2\beta_2^2}{D^2} + 0.20472\frac{R_1^4\beta_1^2 + R_2^4\beta_2{}^2}{D^4} + 0.8598\frac{R_1^2 R_2^2\beta_1\beta_2}{D^4}\right), \quad (14)$$

where $D = s + R_1 + R_2$. s is the distance between two fragments and R_i is the net radius of each deformed fragment which is given as follows:

$$R_i(\theta) = R_{0,i}\sum(1 + \beta_i Y_{i0}(\theta)), \quad (15)$$

where θ is the angle made by the axis of symmetry with fission axis and Y_{i0} is the spherical harmonic function. Also, $R_{0,i}$ is the radius of the nucleus, which can be evaluated using the semi-empirical equation as a function of the mass number of fission fragment as [36,37]

$$R_{0,i}(\mathrm{fm}) = 1.2836A_i^{1/3} - 0.80012A_i^{-1/3} - 0.0021444A_i^{-1}. \quad (16)$$

On the other hand, the fragment intrinsic energy, $E_{\mathrm{int}}(A_i)$, is calculated by

$$E_{\mathrm{int}}(A_i) = a(A_i)\tau_i^2, \quad (17)$$

Table 1. The deformation parameter values of fission fragments for neutron-induced fission of ^{232}Th.

A_i	70–89	89–100	100–104	105	106
β_i	0.65	0.6	0.55	0.51	0.5
A_i	107	108	109	110	111
β_i	0.48	0.44	0.4	0.38	0.36
A_i	112	113	114	115	
β_i	0.35	0.34	0.33	0.32	

where the intrinsic temperature $\tau_i = 41T/2\pi^2 A_i^{1/3}$ [34]. The temperature (T) is calculated with the generalised superfluid model as [38]

$$T = \sqrt{(E_{cn} + E_{\mathrm{pair}} - E_{\mathrm{con}})/a(A_i)}, \quad (18)$$

where E_{cn} is the excitation energy and E_{con} is the condensation energy for the even–even nucleus. We have [38]

$$E_{\mathrm{con}} = \frac{3a}{2\pi^2}E_{\mathrm{pair},0}^2, \quad (19)$$

where $E_{\mathrm{pair},0}(\mathrm{MeV}) = 12/\sqrt{A}$.

3. Results and discussion

Total excitation energy of the fission fragments is calculated for the neutron-induced fission of ^{232}Th using three methods. By comparing the results of the first two methods with the results of the third method, the parameters of the third model are modified. TXE(A) is evaluated and investigated for the other thorium isotopes.

With the exception of ^{232}Th, other thorium isotopes have rarely been studied. In particular, the neutron multiplicity of fission fragments has only been studied for the neutron-induced fission of ^{232}Th. Although the TKE values of fission fragments, TKE(A), have been extensively studied for neutron-induced fission of ^{232}Th, there is no data on the TXE(A) of this reaction. Also, TKE(A) has only been measured for the neutron-induced fission of ^{229}Th and ^{232}Th, and TKE(A) for the other thorium isotopes is evaluated by the scission point model [41]. Since the neutron multiplicity distribution and TKE(A) are measured only for the neutron-induced fission of ^{232}Th, this reaction is first investigated. Then TXE(A) is investigated for the other thorium isotopes.

The total excitation energy in terms of the mass number of the fission fragment for neutron-induced fission of ^{232}Th is presented in figure 1. In Method 1 calculations, the values of total kinetic energy are taken from the experimental data [39]. The binding energy value of the fissioning system and the mass excess values of the fission fragments are taken from [40]. In Method

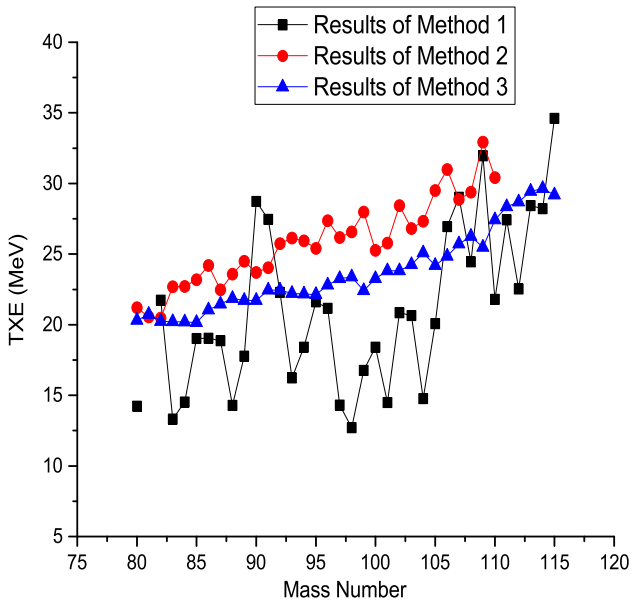

Figure 1. Calculated total excitation energy as a function of fission fragment mass, TXE(A), at 1.6 MeV neutron energy for neutron-induced fission of ^{232}Th.

2, the neutron multiplicity of the fission fragment is taken from [19] and the binding energy values of the fission fragments are taken from [40]. In Method 3, the deformation parameters of the fission fragments, β_i, are required, which are presented in ref. [41]. In this reference, the β_i values for the symmetric region are too large (more than 1). To improve these values, the net radius of each fission fragment is calculated using eq. (15) (as opposed to eq. (7) from ref. [41]) and the β_i values for the symmetric fragments are again calculated using the same method of the mentioned reference. In table 1, the deformation parameters of the fission fragments for neutron-induced fission of ^{232}Th are presented. As can be seen in this table, β_i values are proper for symmetric fragments (i.e., they are less than 1). By these new β_i values, there is a significant difference between the TXE values calculated with the third model and the TXE values calculated with other methods. Wilkins *et al* [42] chose $s = 1.44$ fm, but by choosing $s = 2.88$ fm, TXE values calculated using Method 3 were closer to TXE values calculated using other methods (figure 1).

In figure 1, there are variations in the calculated results using Method 1. These variations are related to rapid changes in the Q-value of fission fragments. While Q-values increase rapidly for complementary fragments with even neutron/proton numbers, variations in the results calculated using Method 1 are related to the odd–even effect. To wash out the odd–even effects, TXE can be calculated with maximum Q-values, such as Nishio calculations for ^{235}U fission [43]. Also, by averaging the TXE values calculated using Method 1, our plots will become smooth. Because the results calculated using Method 3 agree with the results calculated using Method 1, the TXE values calculated using Method 3 can be considered approximately as the average values calculated using Method 1.

Tudora *et al* [44] studied the even–odd effect in total prompt neutron multiplicity. Therefore, variations in TXE values correspond to variations in the total prompt neutron multiplicity. With these variations, the even–odd effect can be investigated. Because the total prompt neutron multiplicity can be calculated by TXE values, variations in TXE values were retained. On the other hand, the impact of Q-value can also be seen on fission fragment mass distribution in ref. [45], where the fission fragments are determined at the highest Q-value. Since the variations are related to Q values, it is not appropriate to eliminate these variations in our TXE results.

From figure 1 it can be seen that the TXE values calculated using Method 1 increase in the symmetric region. This increase in TXE values has been observed in the symmetric region for ^{252}Cf spontaneous fission [17], ^{238}U photofission [46] and ^{233}U and ^{235}U thermal neutron-induced fission [16,18,47]. This increase is related to the decrease in TKE values in this region. On the other hand, TXE values for symmetric fragments were not calculated in some studies [16,43]. There are inconsistencies between TKE data obtained by different experimental groups. These inconsistencies in the experimental data may be due to the thickness of the experimental samples [48]. The increase in TXE values calculated using Method 1 for the symmetric region is greater than the increase in TXE results calculated using Methods 2 and 3 in this region. The TXE results calculated using Method 3 increase slowly with increasing mass numbers of light fission fragments. To fit the TXE values calculated using Method 3 with the results calculated using Method 1, all potential energies in fission process can be considered as the excitation energy (E_{cn}) in eq. (18), such as ref. [23]. Of course, this addition will increase the TXE values for all fission fragments and the difference between the calculated values of the two models will be increased for all fragments. Therefore, it is better to use only the Coulomb energy, which increases more for symmetric fission fragment than for other fission fragments.

Investigating the third method, it can be seen that the share of the deformation energy ($E_{\text{def}} \simeq$15–20 MeV) in TXE is greater than the intrinsic energy ($E_{\text{int}} \simeq$1 MeV). Since E_{def} is proportional to the square of the Coulomb energy (eq. (12)), the increase in TXE values for the symmetric fragments can be due to the Coulomb energy of the fission fragments.

On the other hand, there is a relative reduction for fission fragments with mass numbers between $A_{\text{L}} = 90$

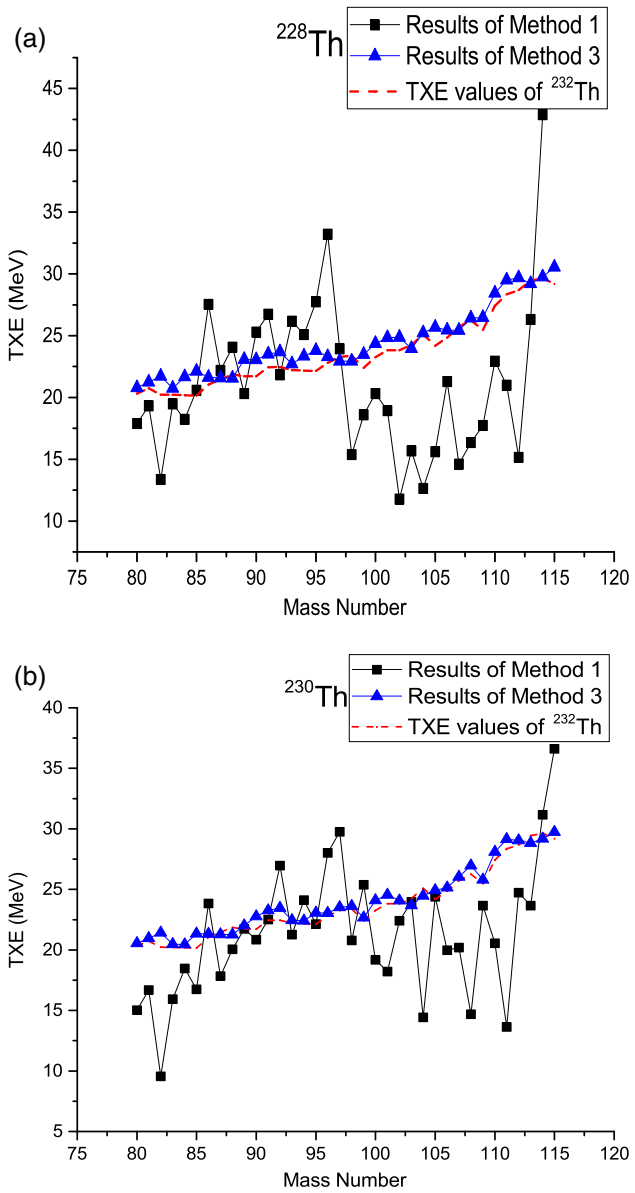

Figure 2. Calculated total excitation energy as a function of fission fragment mass, TXE(A), for thermal neutron-induced fission of (**a**) ^{228}Th and (**b**) ^{230}Th using Methods 2 and 3.

and 105, which can be due to the increase in TKE values for the asymmetric region. Interestingly, Q values also increase in the asymmetric region. This indicates that the increase of TKE values is greater than the increase of Q values in this region. Therefore, the number of neutrons released decreases for this region, which can also be seen in figure 7 from ref. [19] (where the total prompt neutron multiplicity is plotted as a function of fission fragments).

The prompt neutron multiplicity of fission fragments ($\nu(A_i)$) is not provided for other thorium isotopes. Therefore, the TXE values calculated using Method 2 cannot be calculated for other isotopes.

According to ref. [27], there is a large difference between the TKE values of fragments for even and odd isotopes, and also between the deformation parameters of fission fragments for even and odd isotopes. Therefore, the TXE values for neutron-induced fission of odd and even isotopes are calculated separately below.

TXE(A) for neutron-induced fission of even thorium isotopes is presented in figure 2. The deformation parameters of the fission fragments for ^{232}Th fission have been selected as deformation parameters of fission fragments for even thorium isotopes such as ref. [41]. The TKE values of even thorium isotopes are taken from ref. [41].

In figure 2, the results calculated using Method 1 are significantly decreased for fission fragments with mass numbers between 100 and 110 for ^{228}Th and ^{230}Th. Since there are slight differences between the TKE values calculated for the ^{228}Th and ^{230}Th fissions (ref. [41]), the reduction in the TXE values is related to the reduction in Q values. TXE values for ^{228}Th fission in fragments $A = 96$ and 98 are equal to 33.2 and 15.3 MeV, while the TXE values for ^{230}Th fission in fragments $A = 97$ and 98 are equal to 29.7 and 20.7 MeV. Therefore, the reduction rate in TXE values for ^{228}Th fission is greater than the reduction rate in TXE values for ^{230}Th fission. The same behaviour can be seen in the TXE values of ^{230}Th and ^{232}Th fission. Therefore, the reduction rate in TXE values in this region decreases with increasing mass numbers of fissioning systems. On the other hand, the weight of the asymmetric mode of fissioning systems increases with increasing mass numbers. Therefore, the reduction rate in TXE values is related to the symmetric fission mode. Since the fission of the actinides is asymmetric, there is no sharp decrease in the TXE distribution of actinides [16,43,46,47].

The TXE values calculated using Method 1 for ^{228}Th and ^{230}Th fission increase significantly in the symmetric fission fragments ($A_{cn}/2$). Since the increase in TKE values for this region is about 1 MeV [41], the increase in TXE values for the symmetric fragments is due to a decrease in the TKE values and an increase in Q values. The increase in Q values in this region corresponds to the increase in the probability of the formation of symmetric fragments, which is seen in the three-hump mass distributions of thorium isotope fission [49]. The TXE value in the symmetric fragments for ^{228}Th fission is 42 MeV while the TXE value in the symmetric fragment for ^{230}Th fission is 36 MeV. Also, the TXE value in the symmetric fragment for ^{232}Th fission is equal to 34 MeV. This indicates that the TXE value in the symmetric fragment increases with decreasing mass number of the fissioning system.

Comparing figures 2a and 2b, it can be seen that the TXE(A) calculated using Method 3 has the same

behaviour for the neutron-induced fission of ^{230}Th and ^{228}Th. The same behaviour is seen in the ^{232}Th neutron-induced fission (figure 1).

The dash line in figure 2 indicates the TXE values calculated using Method 3 for the neutron-induced fission of ^{232}Th. It can be seen that the TXE values calculated using Method 3 for ^{228}Th fission are greater than the TXE values for ^{232}Th fission. This indicates that the TXE values calculated using Method 3 increase with decreasing mass number of fissioning system.

On the other hand, the values calculated using two methods are very different for fission fragments with mass numbers greater than 96. This difference is observed in both symmetric and asymmetric regions. The difference in TXE values in the asymmetric region can be related to the difference in the deformation parameter values for the asymmetric fission fragments. The difference in TXE values in the symmetric region can be improved by adding effective energies to the excitation energy as mentioned before for ^{232}Th fission.

In figure 3, TXE(A) is presented for neutron-induced fission of odd thorium isotopes. The deformation parameters of fission fragments for odd isotopes are selected as the deformation parameters of ^{229}Th fission. Of course, the deformation parameters of fragments with mass numbers from 116 to 119 are not presented in ref. [41]. We evaluated them using the same method used in this reference. The deformation parameters of fragments with mass numbers from 116 and 119 are 0.88, 0.84, 0.81 and, 0.755, respectively. Also, the TKE values of fragments for ^{229}Th fission are taken from ref. [6] and the TKE values of fragments for other odd thorium isotopes are taken from ref. [41].

In figure 3, The TXE values calculated using Method 1 for all odd isotopes have a considerable reduction in fragments of mass numbers around 100, such as the TXE values of even isotopes. This decrease is noticeable. As the increase in TKE values for this region is about 1 MeV, the decrease in TXE values for the asymmetric region is due to the increase in TKE values and the decrease in Q values. On the other hand, the TXE values in fission fragments with mass numbers 103 and 104 for ^{231}Th fission are less than 15 MeV, while the TXE values in fission fragments with mass numbers $A_{\mathrm{L}} = 99$, 101, 102 and 106 for ^{227}Th fission are less than 15 MeV. The same behaviour can be seen for the fission of even thorium isotopes (i.e., the TXE values in fragments with mass numbers 102, 103–107 and 112 for ^{228}Th fission are less than 15 MeV while the TXE values in fragments with mass numbers 98, 101, 104 for ^{232}Th fission are less than 15 MeV). This indicates that the TXE values for fewer fission fragments is reduced in heavier isotopes. This is due to the increase in Q values in heavy isotopes.

In figure 3, the TXE values calculated using Method 1 increase clearly in the symmetric region. This is due to the decrease in TKE values and the increase in Q values in the symmetric fragments.

The dash line in figure 3 indicates the TXE values calculated using Method 3 for neutron-induced fission of ^{232}Th. In this figure, there is a clear difference between the calculated TXE values using the third method for even isotopes and odd isotopes. This difference is due to the difference in the deformation parameters of the fission fragments of even and odd isotopes.

Also, it can be seen that the TXE values using Method 3 for ^{227}Th fission are greater than the TXE values using Method 3 for ^{232}Th fission. This decrease in TXE values using Method 3 can also be seen for even isotopes (figure 2). This indicates that the TXE values of fragments increase with decreasing mass number of the fissioning system.

The fission fragment mass distribution of $^{227-233}$Th fission has three humps. As the weight of the symmetric mode decreases in heavy isotopes, the probability of the formation of symmetric fragments decreases. This decrease in probability of formation corresponds to a decrease in Q values with increasing mass number of thorium isotopes. This decrease in the Q value can be seen in other studies [50,51]. Therefore, TXE values decrease with increasing mass number of isotopes (figures 1–3).

For fission fragments with mass numbers between 95 and 110, located near the asymmetric region in all thorium isotopes, TXE values are significantly reduced (figures 1–3). This reduction is due to the formation of the fragments with semi-magic and magic atomic number nuclei ($Z_{\mathrm{L}} = 40$, $Z_{\mathrm{H}} = 50$). In semi-magic and magic fragments, the deformation energy is significantly reduced (eq. (11)). Also, the average neutron multiplicity for these shell-closed fragments is reduced [19]. The average neutron multiplicity is foremost a reflection of how much excitation energy is present in the fission fragment from which the neutrons are evaporated [52]. On the other hand, the mass of fission fragment with minimum TXE values increases as the mass number of thorium isotopes increases.

In this study, TXE(A) is calculated for the thorium isotopes with mass numbers greater than 227, because the fission mode changes in the thorium isotopes with mass numbers less than 227. Since TKE values (in Method 1) and the deformation parameters of the fission fragments (in Method 3) depend on the fission mode, TXE(A) for

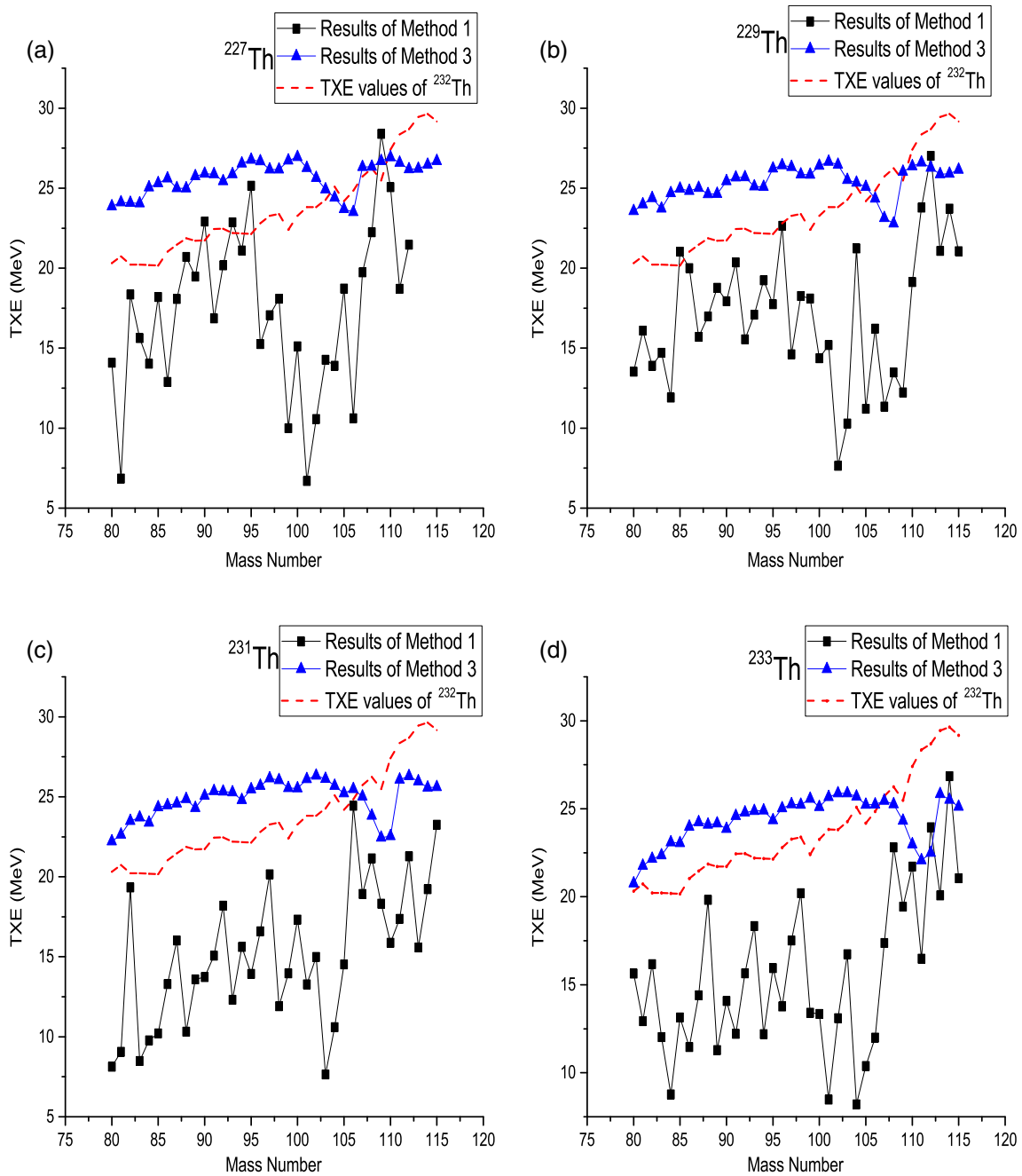

Figure 3. Calculated total excitation energy as a function of fission fragment mass for neutron-induced fission of (**a**) ^{227}Th, (**b**) ^{229}Th, (**c**) ^{231}Th and (**d**) ^{233}Th using Methods 1 and 3.

the thorium isotopes with mass numbers less than 227 cannot be studied by these methods.

In table 2, the minimum and maximum TXE values are presented for thorium, uranium and plutonium isotopes and ^{252}Cf. The fission fragment mass numbers with minimum and maximum TXE values are also presented. These values are taken from refs [43,46,47] for neutron fission of ^{233}U, ^{235}U and ^{238}U, respectively. Also, the minimum and maximum TXE values of plutonium isotopes are taken from Neiler *et al* [18]. The minimum and maximum TXE values for ^{252}Cf fission are taken from Schmitt *et al* [17] and Tudora *et al* [44], separately.

Schmitt *et al* showed that the TXE values calculated using Methods 1 and 2 are the same. Although Tudora *et al* also calculated TXE values using Method 2, their results are very different. For example, although the maximum TXE value in both calculations is 45 MeV, this value occurs in Schmitt calculations for a fragment with mass number 132, while in Tudora calculations it

Table 2. The maximum and minimum TXE values for actinides (MeV).

	^{227}Th	^{228}Th	
$A_i = 101/102$	6.7	11.7	
$A_i = 108/114$	28.3	42	
	^{229}Th	^{230}Th	
$A_i = 102/111$	7.6	13.6	
$A_i = 112/115$	27	36	
	^{231}Th	^{232}Th	^{233}Th
$A_i = 103/98/104$	7.6	12	9.9
$A_i = 106/115/114$	24	34.5	26.8
	^{233}U [47]	^{235}U [43]	^{238}U [46]
$A_i = 88/103/95$	22	21	24
$A_i = A_{cn}/2(108)$	39	(32)	44
	^{239}Pu [18]	^{241}Pu [18]	
A_i =104–106	25	26	
$A_i = A_{cn}/2$	40	39	
	^{252}Cf [17]	^{252}Cf [44]	
$A_i = 102$–3	32	32	
$A_i = 132, A_{cn}/2$	45	45	

occurs in the symmetric fragment ($A = 125$). However, the minimum and maximum TXE values calculated by Schmitt *et al* [17] and Tudora *et al* [44] are the same.

As shown in table 2, the minimum and maximum TXE values for ^{239}Pu fission are greater than these values for ^{241}Pu fission. The minimum and maximum TXE values of ^{233}U fission are also greater than these values for ^{235}U fission. Although Nishio did not provide TXE values for the symmetric fission fragments (which are usually the highest values), the maximum TXE value for neutron fission of ^{233}U is greater than this value for the neutron fission of ^{235}U. Therefore, the minimum and maximum TXE values decrease by increasing the mass number of isotopes. For thorium isotopes, our results have the same behaviour, i.e., the minimum and maximum TXE values increase as the mass number of isotopes decreases.

In addition, in table 2, the minimum and maximum TXE values of ^{238}U photofission are greater than these values for ^{233}U, ^{235}U fission. Also, the minimum and maximum TXE values of ^{252}Cf spontaneous fission are much greater than these values for odd plutonium isotopes. Although there is a significant increase in the minimum and maximum TXE values for photofission of ^{238}U and for spontaneous fission of ^{252}Cf, the calculated minimum and maximum of TXE values for even thorium isotopes are also greater than for odd thorium isotopes. Therefore, the minimum and maximum TXE values for even isotopes are greater than the minimum and maximum TXE values for odd isotopes. This is due to the large increase in TKE values for neutron-induced fission of odd isotopes.

As can be seen in table 2, the minimum and maximum TXE values for ^{239}Pu fission are greater than these values for ^{235}U fission. These values for ^{252}Cf fission are also greater than them for ^{239}Pu fission. Therefore, the minimum and maximum TXE values increase with increasing atomic mass of the fissioning system.

Since the maximum TXE value for photofission of ^{238}U is approximately equal to this value for spontaneous fission of ^{252}Cf, the maximum TXE value for photofission is greater than spontaneous and neutron fission.

Since the maximum TXE value for ^{228}Th fission is greater than the maximum TXE value for ^{227,229,231,233}Th fission, the increase in maximum TXE values due to the pairing effect (odd–even isotopes) is greater than the increase in maximum TXE values due to the mass number.

On the other hand, TXE values are usually maximised in symmetric fission fragments. However, the maximum TXE value for ^{235}U fission occurs in the fragment with mass number 108. This is because the TXE values for the symmetric fission fragment in ref. [43] are not examined. The TXE value in the symmetric fission fragment ($A_{cn}/2$) is not maximised for spontaneous fission of ^{252}Cf and some neutron-induced fission of thorium isotopes. This may be related to the increase in the weight of symmetric mode in these reactions, because there is a

symmetric mode (super-long mode) in the ^{252}Cf spontaneous fission and the mass distributions of thorium isotopes have three humps.

4. Conclusions

The fission fragment total excitation energy for neutron-induced fission of ^{232}Th is investigated using three methods. Unfortunately, the TXE values for other thorium isotopes have not been studied up to now. So TXE(A) for neutron-induced fission of $^{227-233}$Th is evaluated using two methods.

There are variations (fluctuation) in the results calculated using Method 1. These variations are related to rapid changes in the Q value of fission fragments.

The TXE values calculated using Method 1 increase sharply near the symmetric fission fragments. The TXE values calculated using Method 3 increase smoothly with proximity to the symmetric region. Totally, the TXE values using three methods increase with proximity to the symmetric region. This seems to be related to the dominance of the asymmetric mode in actinides fission.

Also, a great reduction of TXE values for fragments with mass numbers about 100–110 can be seen for all thorium isotopes. This reduction is due to the formation of the fragments with semi-magic and magic atomic number nuclei ($Z_{\mathrm{L}} = 40$, $Z_{\mathrm{H}} = 50$). The average neutron multiplicity is foremost a reflection of how much excitation energy is present in the fission fragment from which the neutrons are evaporated.

A systematic method (Method 3) is modified with the TXE results calculated by other methods. Therefore, it is better to add all potential energies in the fission process in the initial excitation energy of fissioning systems (E_{cn}).

The minimum and maximum values of TXE decrease by increasing the mass number of thorium isotopes. This is due a decrease in the Q value with an increase in the mass number of thorium isotopes. Since the weight of symmetric mode decreases in heavy isotopes, the Q values decrease with increasing mass number of thorium isotopes.

Also, the minimum and maximum TXE values for even isotopes are greater than the minimum and maximum TXE values for odd isotopes. Because of one unpaired neutron, neutrons are more easily emitted (evaporated) in odd fissioning systems (the neutron-induced fission of even isotopes) than in even fissioning systems. Since neutron evaporation for the neutron-induced fission of even isotopes is greater than neutron evaporation for the neutron-induced fission of the odd fissioning systems, TXE values for even isotopes are higher than TXE values for odd isotopes. Therefore, in the neutron-induced fission of even isotopes, neutrons emit easily, and so TXE values increase.

Also, the minimum and maximum TXE values increase by increasing the atomic mass of fissioning system.

However, the increase in minimum and maximum TXE values due to the pairing effect is greater than the increase of these values with increasing atomic number.

Neutron multiplicity as a function of fission fragment mass numbers will be evaluated in the next study with the presented TXE values. Also, temperature, level density parameter, deformation energy and deformation parameter of fission fragments can be evaluated by the presented TXE values.

References

[1] S T Lam, L L Yu, H W Fielding, W K Dawson and G C Neilen, *Phys. Rev. C* **28**, 1212 (1983)

[2] J Trochon, H Abou Yehia, F Brisard and Y Pranal, *Nucl. Phys. A* **318**, 63 (1979)

[3] W Holubarsch, E Pfeiffer and F Gbnnenwein, *Nucl. Phys. A* **171**, 631 (1971)

[4] C Budtz-Jorgensen and H H Knitter, *Nucl. Phys. A* **490**, 307 (1988); **491**, 56 (1989)

[5] M Caamano and F Farget, *Phys. Lett. B* **770**, 72 (2017)

[6] J P Unik, J E Gindler, L E Glendenin, K F Flynn, A Gorski and R K Sjoblom, *Proc. Third Symp. on Physics and Chemistry of Fission* (Rochester, 1973) Vol. 2 (IAEA, Vienna, 1974) p. 19

[7] M Asghar *et al*, *Nucl. Phys. A* **373**, 225 (1982)

[8] C Manailescu, A Tudora, F-J Hambsch, C Morariu and S Oberstedt, *Nucl. Phys. A* **867**(**1**), 12 (2011)

[9] H R Faust, *The Eur. Phys. J. A: Hadrons and Nuclei* **14**, 459 (2002)

[10] D G Madland and J Rayford Nix, *Nucl. Sci. Eng.* **81**, 213 (1982)

[11] C Morariu, A Tudora, F J Hambsch, S Oberstedt and C Manailescu, *J. Phys. G: Nucl. Part. Phys.* **39**, 055103 (2012)

[12] A Tudora, F J Hambsch, I Visan and G Giubega, *Nucl. Phys. A* **940**, 242 (2015)

[13] A Tudora, *Ann. Nucl. Energy* **33**, 1030 (2006)

[14] U Brosa *et al*, *Phys. Rep.* **197**, 167 (1990)

[15] A Ruben, H Marten and D Seeliger, *Z. Phys. A* **338**, 67 (1991)

[16] W Lang, H G Clerc, H Wohlfarth, H Schrader and K H Schmidt, *Nucl. Phys. A* **345**, 34 (1980)

[17] H W Schmitt, J H Neiler and F J Walter, *Phys. Rev.* **141**, 1146 (1966)

[18] J N Neiler, F J Walter and H W Schmitt, *Phys. Rev.* **149**, 894 (1966)

[19] I Visan, G Giubega and A Tudora, *Rom. Rep. Phys.* **67**, 483 (2015)

[20] M Jamiati and P Mehdipour Kaldiani, *Turk. J. Phys.* **44**, 364 (2020)
[21] N Carjan, F A Ivanyuk and V V Pashkevich, *Phys. Procedia* **31**, 66 (2012)
[22] F A Ivanyuk, *Phys. Scr.* **89**, 054012 (2014)
[23] P M Kadiani, *Front. Phys.* **9**, 629978 (2021)
[24] P Mehdipour Kaldiani, *Phys. Scr.* **95**, 075306 (2020)
[25] P Mehdipour Kaldiani, *Chin. Phys. C* **45**, 024110 (2020)
[26] P Mehdipour Kaldiani, *Phys. Atom. Nucl.* **84**, 11-17 (2021)
[27] P Mehdipour Kaldiani, *Phys. Rev. C* **102**, 044612 (2020)
[28] N Sugarman and A Turkevich, *Radiochemical studies: The fission product* edited by C D Coryell and N Sugarman (McGraw-Hill, New York, 1951) Vol. 3, p. 1396
[29] H Umezawa, S Baba and H Baba, *Nucl. Phys. A* **160**, 65 (1971)
[30] M Pahlavani and P Mehdipour, *Int. J. Mod. Phys. E* **27**, 1850018 (2018)
[31] J Frehaut, *Neutron gamma competition in fast fission (INDC(NDS)–220)* edited by H D Lemmel (International Atomic Energy Agency (IAEA), 1989)
[32] H Marten, A Ruben and D Seeliger, *Fission energetics and prompt neutron emission*, No. INDC (NDS)–220 (1989)
[33] A V Ignatyuk, G N Smirenkin and A S Tishin, *Sov. J. Nucl. Phys.* **21**, 255 (1975)
[34] F A Ivanyuk, C Ishizuka, M D Usang and S Chiba, *Phys. Rev. C* **97**, 054331 (2018)
[35] J Terrell, in: *Proc. Prompt Neutrons from Fission, IAEA Symposium on Physics and Chemistry of Fission* (Salzburg. Vienna, 1965) Vol. II, p. 3
[36] C Karthika and M Balasubramaniam. *Eur. Phys. J. A* **55**, 59 (2019)
[37] V Y Denisov, *Phys. Rev. C* **91**, 024603 (2015)
[38] M Herman, EMPIRE-3.2 Malta-Modular system for Nuclear Reaction Calculations and Nuclear Data Evaluation, Report INDC (NDS)-0603, BNL-101378-2013 (2013) pp. 56–58
[39] A I Sergachev, V G Vorobeva, B D Kuzminov, V B Mikhailov and M Z Tarasko, *Sov. J. Nucl . Phys.* **7**, 475 (1968); *Yadernaya Fizika* **7**, 778 (1968)
[40] G Audi, A H Wapstra and C Thibault, *Nucl. Phys. A* **729**, 337 (2003)
[41] M Jamiaty, *Phys. Atom. Nuclei* **83**, 803 (2020)
[42] B D Wilkins, E P Steinberg and R R Chasman, *Phys. Rev. C* **14**, 1832 (1976)
[43] K Nishio, Y Nakagome, H Yamamoto and I Kimura, *Nucl. Phys. A* **632**, 540 (1998)
[44] A Tudora *et al*, *Nucl. Phys. A* **929**, 260 (2014)
[45] K P Santhosh and A Cyriac, *Comptes Rendus Phys.* **20**, 569 (2019)
[46] S Pomme, E Jacobs, M Piessens, D De Frenne, K Persyn, K Govaert and M-L Yoneama, *Nucl. Phys. A* **572**, 237 (1994)
[47] K Nishio, M Nakashima, I Kimura and Y Nakagome, *J. Nucl. Sci. Technol.* **35**, 631 (1998)
[48] A Göök, C Eckardt, J Enders, M Freudenberger, A Oberstedt and S Oberstedt, *Phys. Rev. C* **96**, 044301 (2017)
[49] K-H Schmidt *et al*, *Nucl. Phys. A* **665**, 221 (2000); K-H Schmidt *et al*, *Nucl. Phys. A* **693**, 169 (2001)
[50] K P Santhosh and B Priyanka, *Nucl. Phys. A* **940**, 21 (2015)
[51] C Li, J Tian and F Zhang, *Phys. Lett. B* **809**, 135697 (2020)
[52] P Talou *et al*, *The Euro. Phys. J. A* **54**, 9 (2018)